Food Chemistry: X 24 (2024) 101893

Contents lists available at ScienceDirect

Food Chemistry: X

journal homepage: www.sciencedirect.com/journal/food-chemistry-x

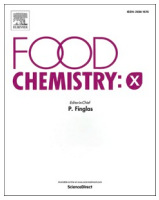

# Multi-omics revealed antibacterial mechanisms of licochalcone A against MRSA and its antimicrobic potential on pork meat

Fei Zeng [a,1], Shijuan Shao [a,1], Zhilu Zou [a], Siqi Guo [a], Yu Cai [a], Chunchao Yan [a], Yunzhong Chen [a], Maolin Wang [b,*], Tingting Shi [c,**]

[a] Faculty of Pharmacy, Hubei University of Chinese Medicine, Wuhan 430070, China
[b] Institute of Traditional Chinese Medicine Health Industry, China Academy of Chinese Medical Sciences, Nanchang 330115, China
[c] Department of Human Anatomy and Histoembryology, Nanjing University of Chinese Medicine, Nanjing 210023, China

ARTICLE INFO

*Keywords:*
Licorice flavonoids
Methicillin-resistant *Staphylococcus aureus*
Micelles
Glycyrrhizin

ABSTRACT

Licorice flavonoids (LFs) exhibit potent antibacterial activities against Gram-positive bacteria. However, the related mechanism remains unclear. This study aims to illustrate the mechanisms of licochalcone A (LA), a main flavonoid in LFs, against methicillin-resistant *Staphylococcus aureus* (MRSA). The anti-MRSA effect of LA was comprehensively investigated by a combination of proteomics and metabolomics studies. Meanwhile, LA was loaded in glycyrrhizin (GA) micelles (GA@LA micelles) to improve its water solubility. The results demonstrated that LA could disrupt the arginine metabolism and cause the accumulation of intracellular ROS in MRSA. In addition, LA could inhibit the expression of glucokinase in MRSA, which affect the synthesis of ATP, fatty acids, and peptidoglycan. GA@LA micelles have the latent ability to inhibit the growth of MRSA on fresh pork.

## 1. Introduction

*Staphylococcus aureus* poses a serious challenge to human health. It can cause various infections, such as skin and soft tissue infections, respiratory tract infections, and urinary tract infections (Cheung et al., 2021). Additionally, *S. aureus* is a major foodborne pathogen that secretes enterotoxins into food, causing acute gastroenteritis in humans and mammals (Papadopoulos et al., 2019). In the past decades, β-lactam antibiotics were effective against *S. aureus* infections. However, due to the misuse of antibiotics in clinics, the drug resistance of pathogenic bacteria is increasing, such as methicillin-resistant *Staphylococcus aureus* (MRSA), which is almost resistant to all β-lactam antibiotics (Hernández-Aristizábal & Ocampo-Ibáñez, 2021). Furthermore, β-Lactam antibiotics are widely used in livestock to promote growth and prevent animal infections. However, their overuse and misuse have led to the emergence of antibiotic-resistant strains of *Staphylococcus aureus*. These resistant strains, particularly MRSA, can spread through the food chain, resulting in contamination of meat and other animal products (da Silva et al., 2020). As MRSA contamination in food becomes increasingly common, it poses a significant threat to public health. This urgent situation calls for a concerted effort to identify and develop new antibacterial agents capable of effectively combating MRSA. Developing antimicrobial compounds is crucial to enhance our ability to prevent MRSA contamination in food products. Such initiatives are vital not only for protecting consumer health but also for ensuring the overall safety and integrity of the food supply chain.

Microbial contamination in foods is prevented using preservatives like sorbate and nitrite, which extend shelf-life and maintain quality. However, long-term consumption of foods containing these chemical components may cause a number of side effects, such as teratogenicity and carcinogenicity (Sun et al., 2023). Therefore, natural preservatives, such as plant and animal-derived products, have attracted significant interest as candidates to inhibit the growth of foodborne pathogens in food (Yu et al., 2021). In China, licorice (known as Gancao) has been used to treat microbial infectious diseases, including respiratory tract infections and urinary tract infections (Sun et al., 2017). It has also been demonstrated that licorice flavonoids (LFs) exhibited potent antibacterial activities against Gram-positive bacteria, especially against MRSA (Zeng et al., 2021). Although LFs showed potent activities against MRSA, the poor solubility of LFs limits their application. Micelles have

* Corresponding author.
** Corresponding author at: Nanjing University of Chinese Medicine, Xianlin Road, Qixia District, Nanjing City, China.
*E-mail addresses:* 17805008158@163.com (M. Wang), 846101@njucm.edu.cn (T. Shi).
[1] Both authors contributed equally to this article.

https://doi.org/10.1016/j.fochx.2024.101893
Received 12 July 2024; Received in revised form 6 October 2024; Accepted 10 October 2024
Available online 11 October 2024

been shown to effectively improve the solubility of lipophilic compounds such as flavonoids and vitamins (Davidov-Pardo et al., 2015). A previous study has demonstrated that glycyrrhizin micelles could improve the solubility of baicalin (Zeng et al., 2022). In addition, licorice extracts containing LFs and glycyrrhizin are widely used in foods due to their broad biological activities and superior safety (Chen et al., 2021).

With the development of proteomic, metabolomic, and transcriptomic technologies, the focus on the actions of antimicrobial agents has gradually shifted from classic specific targets to bacterial metabolic networks. For example, the actions of kurarinon against MRSA using proteomics and metabolomics, in which kurarinon could affect the energy metabolism and biofilm synthesis in MRSA by inhibiting its amino acid metabolism (Weng et al., 2023). Based on the structural similarity between kurarinon and LFs, the mechanism of LFs against MRSA were illustrated by integrating proteomics and metabolomics. First, the structure-activity relationship of LFs against MRSA was investigated to select the optimal antibacterial agents in LFs. Then, licochalcone A (LA), which was abundant in LFs and showed potent activities against MRSA, was selected for further study, where the actions of LA against MRSA were illustrated using multi-omics. Furthermore, glycyrrhizin micelles were used as carriers to improve the solubility of LA. Meanwhile, LA-loaded glycyrrhizin micelles were used to prevent fresh pork contamination caused by MRSA.

## 2. Materials and methods

### 2.1. Reagents

3,3-dipropylthiadicarbocyanine iodide [DiSC3(5)] was purchased from Yuanye Technology Co. Ltd. (Shanghai, China). Glutaraldehyde and propidium iodide (PI) were purchased from Shanghai Aladdin (Shanghai, China). Phosphatidylglycerol, phosphatidyl-ethanolamine, cardiolipin, formic acid, iodoacetamide, dithiothreitol, carbamide, protease inhibitor, and triethylammonium bicarbonate were obtained from Sigma-Aldrich (St. Louis, USA). The reactive oxygen species kit and bacterial total RNA extraction kit were supported by Nanjing Jiancheng Bioengineering Institute (Nanjing, China). ATP assay kit and bicinchoninic acid (BCA) protein quantification kit were purchased from Beyotime Biotechnology (Nanjing, China). cDNA synthesis kit and PCR fluorescent quantification kit were provided by TransGen Biotech (Beijing, China). PCR primers were provided by Sangon Biotech (Shanghai, China).

### 2.2. Antibacterial tests

The strains included MRSA-BH, MRSA-ZH, and USA 300, where MRSA-BH and MRSA-ZH were isolated from clinical samples and supported by Nanjing Medical University (Nanjing, China). USA300 was supported by Fenghai Biotech (Hangzhou, China). The minimum inhibitory concentrations (MICs) of compounds were determined according to the previous study(Andrews, 2001). Briefly, the tested compounds were diluted in dimethylsulphoxide (DMSO) to obtain an initial concentration of 1 g/L. Then, 100 μL of initially prepared sample solution was added into the first well, and the sample was then diluted through the serial two folds dilutions. Furthermore, bacteria were adjusted to $10^6$ CFU/mL, and 100 μL of diluted bacteria was then added into every well. The bacteria were incubated at 37 °C for 18 h. After incubating at 37 °C for 18 h, the minimum inhibitory concentrations of tested samples were calculated.

### 2.3. Time-kill curves

Time-kill curves of licochalcone A (LA) were determined according to the previous study (Soontornpas et al., 2005). Briefly, the bacteria ($10^6$ CFU/mL) were treated with different final concentrations of LA (1 MIC, 2 MIC and 4 MIC) and incubated at 37 °C for 2 h, 4 h, 6 h, 8 h, 12 h, and 24 h, respectively. Colonies in each spot were counted and the time killing curves were constructed by plotting mean colony counts (log CFU/mL, taking into account the dilution factors) versus time.

### 2.4. Morphological analysis

The effects of LA on MRSA microstructures were observed using an emission scanning electron microscope (SEM), according to the previous study (**Otto et al.,** 2010). Briefly, the bacteria were first incubated with LA (2 MIC) at 37 °C for 2 h. The bacteria were collected by centrifugation at 5000*g* for 10 min and washed three times with phosphate buffered saline (PBS) (0.01 mol/L pH 7.4). The bacteria were then fixed with 25 g/L glutaraldehyde for 2 h and washed three times with PBS, f followed by dehydration with 30 % (*v*/v), 50 % (v/v), 70 % (v/v), 90 %(v/v), and 100 % (v/v) ethanol.

### 2.5. Membrane integrity assays

The propidium iodide (PI) fluorescent probe was used to evaluate the effects of LA on the cell membrane integrity, according to the previous study (Lunde et al., 2009). The bacteria were first incubated with LA at 37 °C for 2 h. The bacteria were collected by centrifugation at 5000*g* for 10 min and washed three times with PBS (0.01 mol/L, pH 7.4). The bacteria were then mixed with 10 μL of PI (1 mg/L) at 37 °C for 30 min. After incubation, the bacteria were collected by centrifugation at 5000*g* for 10 min and then washed with PBS (0.01 mol/L, pH 7.4) three times. The fluorescence values were determined by using a multimode reader at an excitation wavelength of 535 nm and an emission wavelength of 615 nm.

### 2.6. Membrane potential assay

The DiSC3(5) fluorescent probe was used to evaluate the effects of LA on the membrane potential assay, according to the previous study (Lunde et al., 2009). Bacteria were collected by centrifugation at 5000*g* for 10 min and washed three times with PBS (0.01 mol/L, pH 7.4). The bacteria were mixed with 10 μL of DiSC3(5) (1 mg/L) at 37 °C for 30 min and then incubated with LA at 37 °C for 2 h. After incubation, the bacteria were collected by centrifugation at 5000*g* for 10 min and then washed three times with PBS (0.01 mol/L, pH 7.4). The fluorescence values were determined by using a multimode reader at an excitation wavelength of 622 nm and an emission wavelength of 670 nm (Enspire, Perkin Elmer, Waltham, MA, USA).

### 2.7. ATP determination

The effects of the compound on bacterial intracellular ATP were evaluated using the ATP Assay Kit according to the manufacturer's instructions. Bacteria were collected by centrifugation at 5000*g* for 10 min and washed three times with PBS (0.01 mol/L, pH 7.4). The bacteria were incubated with different concentrations of LA (1/2 MIC, 1 MIC, 2 MIC, and 4 MIC) at 37 °C for 2 h. After incubation, the bacteria were collected by centrifugation at 5000*g* for 10 min and then washed three times with PBS (0.01 mol/L, pH 7.4). Then, the intracellular ATP of MRSA was determined by chemiluminescence method according to the manufacturer's instructions.

### 2.8. Reactive oxygen species (ROS) determination

The effects of the compound on ROS production in MRSA were evaluated using a DCFH-DA fluorescent probe, according to the previous study (Su et al., 2009). 10 μL of DCFH-DA (10 mg/L) was mixed with bacteria and incubated at 37 °C for 30 min. The bacteria were incubated with different concentrations of LA (1/2 MIC, 1 MIC, 2 MIC, and 4 MIC) at 37 °C for 2 h. After incubation, the bacteria were collected by

centrifugation at 5000*g* for 10 min and then washed three times with PBS (0.01 mol/L, pH 7.4). The fluorescence values were determined by using a multimode reader at an excitation wavelength of 488 nm and an emission wavelength of 525 nm (Enspire, Perkin Elmer, Waltham, MA, USA).

### 2.9. Exogenous addition of amino acids

Arginine, citrulline, and glutamate were mixed with LA to evaluate the effects of amino acids on LA's antibacterial activities. Briefly, amino acids were first dissolved in the medium to obtain an initial concentration of 2 g/L. The different concentrations of amino acids (0–0.5 g/L) were then mixed with LA, and the antibacterial activities were then determined using the broth microdilution method, according to the previous study (Qu et al., 2020).

### 2.10. Multi-omics

#### 2.10.1. Comparative proteomic analysis

Bacteria were incubated with LA (2 MIC) at 37 °C for 2 h and then collected by centrifugation at 5000*g* for 10 min. The bacteria were then mixed with 400 μL of lysis buffer (8 mol/L urea, 1 % protease inhibitor and 2 mmol/L EDTA) on the ice and homogenized by ultrasonication for 5 min. After centrifugation, the concentration of protein was measured using the bicinchoninic acid (BCA) protein quantification kit.

The protein was mixed with dithiothreitol (final concentration of 5 mmol/L), and the solution was incubated at 56 °C for 30 min. Iodine acetamide (IAA) was then added to obtain the final concentration of 11 mmol/L, and the solution was incubated at room temperature without light. The trypsin was added with a ratio of 1:50 (protease: protein, m/m) and then incubated at 37 °C for 12 h.

Chromatographic separations were performed on an ultra-high-performance liquid chromatography system (EASY-NLC 1000, Thermo Fisher, Waltham, MA, USA). The A mobile phase system contains 0.1 % formic acid and 2 % acetonitrile, and the B mobile phase system contains 0.1 % formic acid and 90 % acetonitrile. The gradient program was applied as the following: 0–26 min, 6 %–23 % B; 26–34 min, 23 %–35 % B; 34–37 min, 35 %–80 % B; 37–40 min, 80 % B. The flow rate was maintained at 400 nL/min.

Peptides were then analyzed on MS (Q Exactive™ Plus, Thermo Fisher, Waltham, MA, USA). The electrospray voltage was set as 2.0 KV. The *m/z* scan range was set as 350–1800, and the scan resolution was set as 70,000. After the MS analysis, 20 peptide segments that possessed high signal intensity were selected for MS/MS analysis. The fixed first mass was set as 100 m/z, and the scan resolution was set as 17,500. The automatic gain control (AGC) was set as $5E^4$. The database from Uniprot was set as *Staphylococcus_aureus*_1280.

#### 2.10.2. Metabolomic analysis

Bacteria were incubated with LA (2 MIC) at 37 °C for 2 h and then collected by centrifugation at 5000*g* for 10 min. Then, 100 μL of bacteria was mixed with 500 μL of 80 % methanol (*v*/v) under ultrasonication for 30 min. After centrifugation at 1448*g* for 15 min, 200 μL of sample was mixed with 5 μL of dichlorophenylalanine (1 g/L), which was used as the internal standard for the LC-MS analysis.

Chromatographic separations were performed on an ultra-high-performance liquid chromatography system (Waters, Milford, MA, USA). A mobile phase system included 0.05 % formic acid in $H_2O$ (A) and acetonitrile (B). The gradient program was as follows: 0–1 min, 95 % A; 1–12 min, 95 %–5 % A; 12–13.5 min, 5 % A; 13.5–13.6 min, 5 %–95 % A; 13.6-16 min, 95 % A. The flow rate was maintained at 300 nL/min. The MS analysis was performed on a Q-Exactive Orbitrap mass spectrometer (Thermo Fisher, Waltham, MA, USA). The parameters in positive electron spray ionization ($ESI^+$) were set as follows: Heater Temp 300 °C; Sheath Gas Flow rate, 45 Arb (Arb, atmosphere absolute); Aux Gas Flow Rate, 15 Arb; Sweep Gas Flow Rate, 1 Arb; spray voltage, 3.0 kV. Meanwhile, the parameters in $ESI^-$ were set as follows: Heater Temp 300 °C; Sheath Gas Flow rate, 45 Arb; Aux Gas Flow Rate, 15 Arb; Sweep Gas Flow Rate, 1 Arb; spray voltage, 3.2 kV.

### 2.11. RT-PCR analysis

Bacteria was incubated with LA (2 MIC) at 37 °C for 2 h. After centrifugation at 1448*g* for 15 min, the RNA was extracted using the total RNA extraction kit according to the manufacturer's instructions. The reverse transcription reaction system solution, including 10 μL 2 × ES Reaction Mix, 1 μL Oligo (dT)18, 1 μL RI Enzyme Mix, and 1 μL gDNA Remover was prepared, and cDNA was then synthesized according to the manufacturer's instructions. The TOP Green solution, including 10 μL 2 × Top Green Mix, 0.5 μL Forward Primer, 0.5 μL Reverse Primer, 4 μL cDNA, and 5 μL $ddH_2O$, was prepared and used for the fluorescence quantitative analysis. The mRNA relative level of the gene was then calculated by the $2^{-\triangle\triangle}$Ct method, and 16sRNA was used as an internal reference gene. The primer sequences of different genes used in the present study were listed in Table S1 (shown in supplementary material).

### 2.12. Preparation of micelles

According to a previous study with some modifications (Zhu et al., 2014), the micelles was carried out by using the thin film dispersion method. In brief, glycyrrhizin (150 mg) and LA (20 mg) were first dissolved in 20 mL of 70 % (*v*/v) ethanol, and the mixture was incubation at 60 °C for 10 min. Then, the solvents were removed by using the rotary evaporator to obtain film of LA loaded in glycyrrhizin. To obtain a micellar solution, the hydration of micelles with deionized water was carried out by using the rotary evaporator for 30 min at 60 °C.

### 2.13. Structural characterization of micelles

According to a previous study with some modifications (Zhu et al., 2014), the LA (GA@LA) micelle were determined by using Nano ZS Zetasizer and Mastersizer 3000 (Malvern Instruments Ltd., Worcestershire, UK). The microstructures of micelles were observed using transmission electron microscopy (Zeiss, Oberkochen, Germany).

### 2.14. Evaluating antibacterial activities of micelles

Firstly, GA micelle and GA@LA micelle were added to the Luria-Bertani (LB) medium with 10 g/L or 50 g/L of final concentrations, respectively. The diluted bacteria ($10^6$ CFU/mL) were then coated on an LB medium plate and incubated at 37 °C for 18 h.

### 2.15. Effects of micelles on fresh pork preservation

The fresh pork was first washed three times using deionized water and was then exposed to ultraviolet radiation for 30 min at the super clean bench. The pork was coated with diluted bacteria ($1.0 \times 10^6$ CFU/mL) and then mixed with GA and GA@LA micelle, respectively. After incubation at 4 °C for 3 days, 5 days, and 7 days, the number of MRSA on pork was calculated by plate count. Briefly, the fresh pork was cut into pieces (about 1 cm*1.5 cm), and the pork were then divided into three groups (five pieces per group). In each group, one piece of pork was used for taking photos, and others were used to count the bacteria. At day 3, 5 and 7, one piece of pork was used for counting the bacterial, where meat was washed by 1 mL of sterilized water. The bacteria were ten-fold serially diluted and plated on LB plates to calculate the CFUs after incubation at 37 °C for 18 h.

## 3. Results and discussions

### 3.1. Structure-activity relationship (SAR) of licorice flavonoids against MRSA

As shown in Table 1, the SAR of licorice flavonoids against MRSA was first evaluated. Compared with liquiritigenin (MIC >250 μg/mL), naringenin (MIC >250 μg/mL), and 7,4′-dihydroxyflavone (MIC >250 μg/mL), isoliquiritigenin and echinatin showed activities against MRSA with MIC of 62.5 μg/mL, indicating that chalcones possessed better antibacterial activities than dihydroflavones and flavones. Compared with echinatin (MIC = 62.5 μg/mL), LA, licochalcone D and licochalcone E showed potent activities against MRSA with MICs of 7.8 μg/mL, indicating that the presence of isopentenyl group could enhance the antibacterial activities of chalcone. Taken together, the presence of the isopentenyl group significantly improved the antibacterial activities of chalcones. Therefore, to elucidate the mechanism of isopentenyl chalcones against MRSA, LA, which is the most abundant isopentenyl flavonoid in *Glycyrrhiza inflata*, was selected for further study.

### 3.2. Effects of LA on the cell membrane

The effects of LA on USA300 cell membrane were first evaluated by using SEM (shown in Fig. 1A and Fig. 1B). Compared with the control group, the cells treated with LA became abnormal and thinner, indicating that LA might cause damage to the cell wall or cell membrane. The integrity of the cell membrane is usually evaluated using a propidium iodide (PI) probe, which penetrates the damaged cell membrane and bind with DNA. Thus, the fluorescence intensity (FI) reflects the integrity of the cell membrane (Lunde et al., 2009). As shown in Fig. 1C, FI was constantly increased with the concentration of LA ranging from 1/2 MIC to 4 MIC, indicating that LA could damage the MRSA cell membrane in a dose-dependent manner. When the integrity of the cell membrane is destroyed, membrane potential ($\Delta\psi$) and osmotic pressure are also altered. The fluorescent DiSC3(5) probe was thus used to evaluate the effects of LA on membrane potential. FI was decreased with the concentration of LA ranging from 1/2 MIC to 4 MIC (shown in Fig. 1D). LA could destroy the integrity of the cell membrane and influence the membrane potential of MRSA.

### 3.3. Effects of LA on carbohydrate metabolism

The time-kill curves of LA were described to illustrate further the effects of LA against USA300. As shown in Fig. 1F, the number of viable bacteria decreased sharply after treatment with LA for 2 h, indicating that LA possessed rapid antibacterial activities against MRSA. To elucidate the mechanisms of LA against MRSA, the changes in cellular metabolites of MRSA treated by LA for 2 h were analyzed using the metabolomics method based on LC-Q-TOF-MS/MS. As shown in Fig. 2A and B, the major differentiated metabolites (DMs) were selected according to the OPLS-DA model. The major DMs consisted of amino acids and fatty acids (Fig. 2C), and the KEGG pathway enrichment mainly include amino acid and fatty acid metabolism pathway (Fig. 2E). Meanwhile, the changes in the cellular proteome of MRSA treated by LA for 2 h were analyzed using a label-free quantitative proteomic technique. As shown in Fig. 4A, there was a great difference between control and treatment group. Fifty-seven differentially expressed proteins (DEPs), including 41 up-regulated proteins and 16 down-regulated proteins (shown in Fig. 4B). The major DEPs were listed in Table 2, where the fold-change value was over 1.5 or under 1/1.5 (Ratio = LA/Control, $P < 0.05$). As shown in Fig. 4C, the clusters of orthologous groups (COG) analysis indicated that the DEPs were involved in energy production and conversion, transport and metabolism of carbohydrates and amino acids. Furthermore, as shown in Fig. 4D, the DEPs were mainly involved in amino acid and carbohydrates metabolism, fatty acid metabolism. LA had effects on MRSA carbohydrate metabolism, amino acid metabolism, fatty acid metabolism.

With the gradual increase of LA concentration, the ATP level in MRSA gradually decreased (shown in Fig. 1E), indicating that LA might inhibit MRSA carbohydrate metabolism in a dose-dependent manner. Oxidative phosphorylation of glucose is the primary way to obtain energy in microorganisms. The phosphotransferase system is responsible for the transport and phosphorylation of carbohydrates, which are composed of phosphate transfer protein (EI and HPr) and sugar-specific complex (EIIA, EIIB, and EIIC) (Kang et al., 2019). The proteomic results (shown in Table 2) showed that the level of PTS sugar transporter EIIC, phosphate hexose transporter protein (UhpT), and transketolase was significantly increased after treatment with LA ($P < 0.05$). The levels of fructose 1,6-diphosphate, acetyl-CoA, citric acid, α-Ketoglutaric acid, fatty acids and UDP-*N*-acetylglucosamine were significantly decreased in MRSA, after being treated by LA ($P < 0.001$, Fig. 3B and D).

Fructose 1,6-diphosphate (FDP) is a crucial product in the embden meyerhof pathway (EMP), and the level of FDP is closely related to this process (Ning et al., 2021). The level of FDP in the treated group was significantly decreased ($P < 0.001$, Fig. 3D), indicating that LA might inhibit the EMP of MRSA. When EMP is inhibited, the microorganism will activate the hexose monophosphate pathway (HMP) to acquire more ATP (Cheng et al., 2017). Acetyl-CoA, which is mainly produced by the oxidative decarboxylation of pyruvate, is an essential precursor for the synthesis of fatty acids in microorganisms (Parsons & Rock, 2011). When the EMP was inhibited, HMP would be activated to produce the pyruvate, which could compensate for the deficiency of acetyl-CoA in microorganisms(Vimala & Harinarayanan, 2016). Transketolase (TK), which is responsible for the transportation of ketone alcohol groups in HMP, is a characteristic enzyme (Vimala & Harinarayanan, 2016). The level of TK in MRSA treated with LA was significantly increased, indicating that the HMP of MRSA was activated after treatment with LA, while the EMP of MRSA might be inhibited by LA. Furthermore, the level of acetyl-CoA was significantly decreased in MRSA after treatment with LA (shown in Fig. 3D). Acetyl-CoA is an essential precursor for the tricarboxylic acid cycle (TCA). The level of citric acid and α-Ketoglutaric acid were also significantly decreased in MRSA treated by LA, indicating that LA inhibited TCA of MRSA. This may be related to the fact that the EMP in MRSA was inhibited by LA, which caused a decrease in the production of acetyl-CoA. Therefore, inhibition of fatty acid synthesis and TCA in MRSA might be caused by the inhibition of EMP.

The cell wall of Gram-positive bacteria, which is mainly composed of peptidoglycan, plays a vital role in maintaining the morphology and integrity of cells (Vollmer et al., 2008). Under the catalysis of *N*-

**Table 1**
The MICs of licorice flavonoids against MRSA.

| Compounds | Chemical families | MICs (μg/mL) | | |
|---|---|---|---|---|
| | | MRSA-BH | MRSA-ZH | USA300 |
| isoliquiritigenin | chalcone | 62.5 | 62.5 | 62.5 |
| echinatin | chalcone | 62.5 | 62.5 | 62.5 |
| licochalcone A | chalcone | 7.8 | 7.8 | 7.8 |
| licochalcone B | chalcone | 62.5 | 62.5 | 62.5 |
| 2-hydroxy-4,4′-dimethoxychalcone | chalcone | >250 | >250 | >250 |
| tetrahydromethoxychalcone | chalcone | 62.5 | 62.5 | 62.5 |
| licochalcone D | chalcone | 7.8 | 7.8 | 7.8 |
| licochalcone E | chalcone | 7.8 | 7.8 | 7.8 |
| liquiritigenin | dihydroflavone | >250 | >250 | >250 |
| naringenin | dihydroflavone | >250 | >250 | >250 |
| licoisoflavone B | isoflavone | 7.8 | 7.8 | 7.8 |
| glabrone | isoflavone | 15.6 | 15.6 | 15.6 |
| licoricone | isoflavone | 31.2 | 31.2 | 31.2 |
| formononetin | isoflavone | >250 | >250 | >250 |
| 7,4′-dihydroxyflavone | flavone | >250 | >250 | >250 |
| penicillin | | 31.2 | 31.2 | 31.2 |

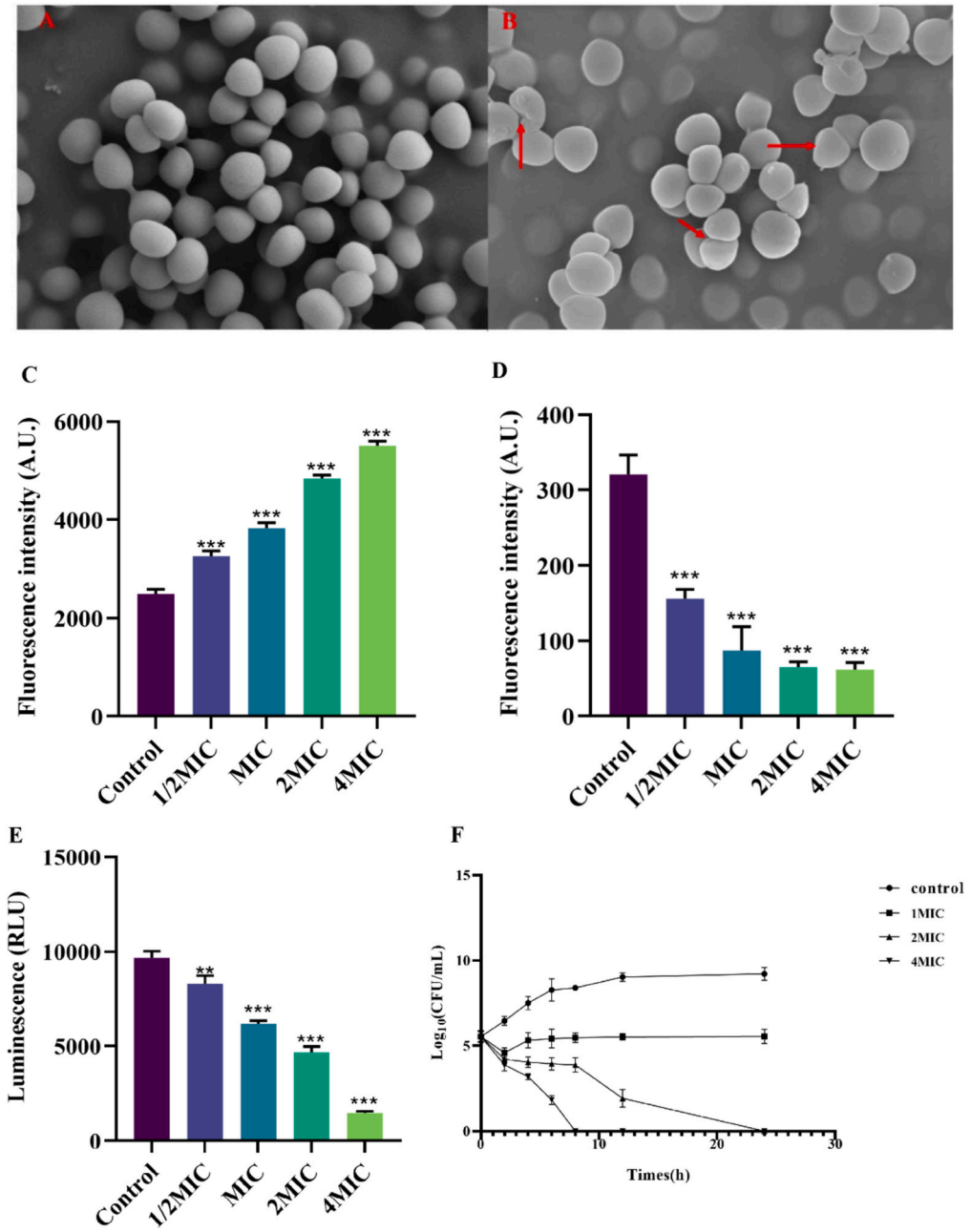


**Fig. 1. The effects of LA on MRSA cell membrane.** (**A–B**) The SEM image of control (**A**) and MRSA treated by LA (**B**), where MRSA treated by LA was characterized by irregular depressions and surface (shown in red arrows); (**C**) The effects of LA on membrane integrity; (**D**) The effects of LA on membrane potential; (**E**) The effects of LA on the production of ATP in MRSA; (**F**) Time-kill curves of LA; ***$P < 0.001$, LA group vs control group. (For interpretation of the references to colour in this figure legend, the reader is referred to the web version of this article.)

acetylglucosamine enolpyruvate transferase and UDP-*N*-glucosamine enolpyruvate reductase, UDP-*N*-acetylglucosamine could be converted to UDP-*N*-acetylmuriatic acid, which is an essential precursor for the synthesis of peptidoglycan in Gram-positive bacteria (Kim et al., 2015). However, the level of UDP-*N*-acetylglucosamine was decreased in MRSA treated with LA, indicating that LA might inhibit the synthesis of UDP-*N*-acetylglucosamine in MRSA. F6P is a crucial precursor for the synthesis of UDP-*N*-acetylglucosamine. Therefore, LA might inhibit the production of F6P, causing a decrease in the production of UDP-*N*-acetylglucosamine. To further illustrate how LA affects the EMP of MRSA, the effects of LA on the expression of essential genes in EMP by using RT-PCR. LA could significantly inhibit the expression of glucokinase (shown in Fig. 3F). Taken together, LA could affect the fatty acids, ATP, and peptidoglycan synthesis in MRSA by inhibiting the EMP of MRSA, in which LA strongly inhibited the expression of glucokinase.

### 3.4. *Effects of LA on amino acid metabolism*

The arginine metabolism in bacteria mainly involves three processes: urea cycle, nitric oxide synthesis, and polyamine synthesis (Cunin et al., 1987). Numerous bioactive molecules are generated during these metabolic processes, which are essential in maintaining the normal physiological activities of bacteria. When bacteria deal with oxidative stress, arginine is converted into nitric oxide, which acts as a signaling molecule to regulate bacterial oxidative stress response and repair oxidative damage (Sudhamsu & Crane, 2009). Furthermore, under oxidative stress, arginine is converted into polyamines such as putrescine and spermidine, which can directly eliminate the reactive oxygen

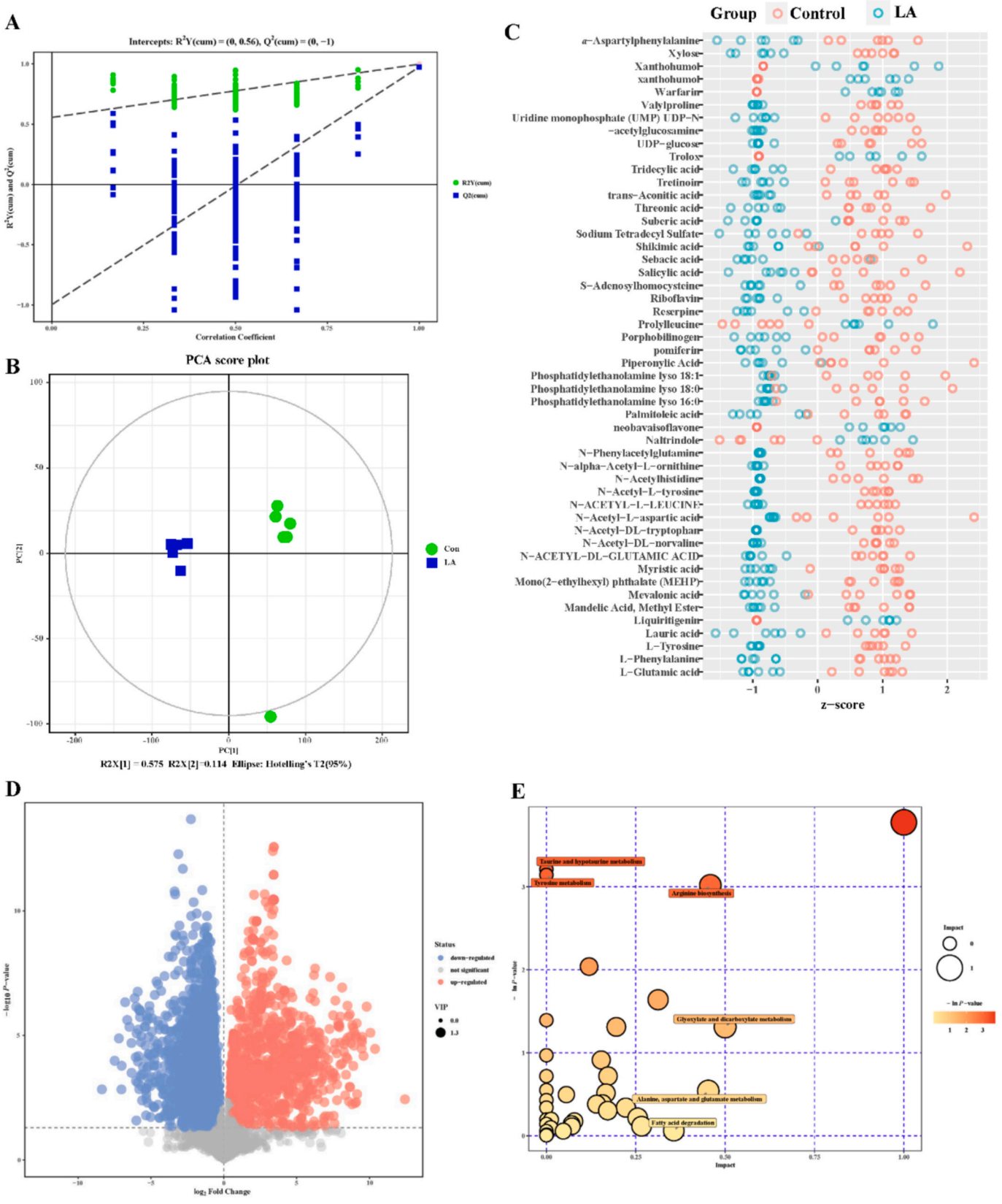


**Fig. 2.** (**A**) The score scatter plot of OPLS-DA, where control group is shown in green symbol and LA group is blue symbol; (**B**) The permutation test of the OPLS-DA **(C)** The metabolomic profiling of MRSA treated by LA **(D)** The volcano plot of differential metabolites (**E**) The KEGG pathway analysis of differential metabolites. (For interpretation of the references to colour in this figure legend, the reader is referred to the web version of this article.)

**Table 2**
The major differential proteins.

| Protein symbol | Protein description | Ratio | *P* value |
|---|---|---|---|
| Adh | Alcohol dehydrogenase | 0.486 | <0.001 |
| PflB | Formate *C*-acetyltransferase | 0.642 | <0.001 |
| SAKOR_01367 | PBS lyase HEAT-like repeat protein SakoR | 1.816 | <0.001 |
| ST398NM01_0162 | Aldehyde-alcohol dehydrogenase | 0.421 | <0.001 |
| E5491_12165 | DUF1542 domain-containing protein | 1.601 | 0.03 |
| Lip2 | Triacylglycerol lipase | 3.228 | <0.001 |
| FPP09_01715 | AAA family ATPase | 1.612 | 0.003 |
| ST398NM01_2664 | Anaerobic ribonucleoside-triphosphate reductase | 0.512 | 0.027 |
| PurA | Carbamate kinase | 0.547 | <0.001 |
| ST398NM01_1163 | Ornithine carbamoyltransferase | 0.369 | <0.001 |
| ST398NM01_1164 | Carbamate kinase | 0.417 | <0.001 |
| BSZ10_04760 | Histidine-containing protein | 1.539 | <0.001 |
| UhpT | Hexose phosphate transport protein | 1.818 | 0.005 |
| FVP29_05690 | PTS sugar transporter subunit IIC | 1.659 | 0.002 |
| E5491_02095 | SDR family oxidoreductase | 0.611 | 0.002 |
| Tkt | Transketolase | 1.614 | 0.015 |
| InfB | Translation initiation factor IF-2 | 6.756 | <0.001 |
| NCTC10702_03190 | Putative phage anti-repressor protein | 1.756 | <0.001 |
| SAKOR_00796 (homologue of CspA) | Cold shock protein CspA | 1.957 | 0.002 |
| CspA | Cold shock protein CspA | 2.017 | 0.0012 |
| Sin | Recombinase Sin | 0.395 | <0.001 |
| ST398NM01_0871 | Micrococcal nuclease | 3.944 | <0.001 |
| E3A28_14150 | Transposase | 0.549 | 0.001 |
| Sle1 | *N*-acetylmuramoyl-L-alanine amidase sle1 | 1.733 | 0.038 |
| Sbi | Immunoglobulin-binding protein Sbi | 2.228 | <0.001 |
| SdrE | MSCRAMM family adhesin SdrE | 1.671 | <0.001 |
| E5491_02095 | SDR family oxidoreductase | 0.611 | 0.002 |
| SdrD | MSCRAMM family adhesin SdrD | 1.626 | <0.001 |
| G6Y30_06790 | LysM peptidoglycan-binding domain-containing protein | 1.612 | 0.003 |
| IsdA | LPXTG-anchored heme-scavenging protein IsdA | 0.624 | 0.033 |
| ORF242 | Uncharacterized protein | 1.51 | 0.003 |
| IsaA | Probable transglycosylase IsaA | 1.764 | <0.001 |
| E5491_14890 | Amidase domain-containing protein | 2.345 | <0.001 |
| G0X15_06680 | Phage major capsid protein | 1.537 | 0.002 |
| BSZ10_09780 | t(6)A37 threonylcarbamoyladenosine biosynthesis protein TsaE | 1.996 | 0.004 |
| G0V60_12460 | CHAP domain-containing protein | 1.721 | 0.007 |
| SAV1707 | UPF0173 metal-dependent hydrolase SAV1707 | 2.107 | <0.001 |
| RpoY | DNA-directed RNA polymerase subunit epsilon | 2.211 | <0.001 |
| ST398NM01_0296 | SsaA | 1.653 | 0.005 |
| E5491_14890 | Amidase domain-containing protein | 2.345 | <0.001 |

species (ROS) in bacteria (Michael, 2018). Meanwhile, polyamines can promote the formation of MRSA biofilms may not be familiar with. Arginine deiminase (AD), ornithine carbamyl transferase (OC), and ornithine decarboxylase (OD) are critical enzymes in the urea cycle, which play a vital role in arginine metabolism. AD, OC, and OD are encoded by the *arc* gene cluster, which is regulated by arginine repressor (ArgR) (Cheng et al., 2017). The transcription factor ArgR needs to be activated by arginine (Qu et al., 2020). The levels of AD, OC, and OD were decreased in MRSA treated with LA, indicating that the synthesis of arginine in MRSA might be inhibited after being treated with LA. Furthermore, the metabolomic results (shown in Fig. 3D) showed that the level of arginine, glutamate, and citrulline in MRSA was sharply decreased after treatment with LA. In bacteria, glutamate and citrulline are significant sources of nitrogen nutrition for synthesizing arginine. Thus, the biosynthesis of arginine in MRSA might be inhibited after treatment with LA.

Flavonoids such as isobavachalcone and kurarinon could cause the accumulation of intracellular ROS (Song et al., 2021). The production of ROS in MRSA treated by LA was measured using a DCFH-DA fluorescent probe. FI was increased with the concentration of LA ranging from 1/2 MIC to 4 MIC, indicating that LA could cause the accumulation of ROS in MRSA in a dose-dependent manner (shown in Fig. 3E). Meanwhile, RT-PCR analysis (shown in Fig. 3F) indicated that the expression of genes related to oxidative stress including *danE* and *groeL* was remarkably up-regulated, indicating that MRSA experienced oxidative damage and DNA damage after being treated by LA. The oxidative damage in MRSA might be related to the dysfunction of arginine metabolism.

The arginine metabolism deficient strain was constructed by using the homologous recombination (Fig. 5A), in which the gene of *argR* in USA300 was deleted. The identification of USA300*ΔargR* was assessed by PCR analysis (Fig. 5B and C). To verify the effect of LA on the arginine metabolism in MRSA, arginine, glutamate, and citrulline were added to the medium. The results (shown in Fig. 5D) indicated that the exogenous addition of arginine and citrulline could enhance MICs from 7.8 μg/mL to 15.6 μg/mL. The exogenous addition of arginine and citrulline has no effects on the MIC of LA against USA300△*argR*. The activities of LA against MRSA might be related to its inhibition of the biosynthesis of arginine in bacteria, which caused the dysfunction of arginine metabolism. Taken together, LA inhibited the expression of glucokinase in EMP, resulting in the inhibition of oxidative phosphorylation of glucose, fatty acids, and peptidoglycan synthesis. In addition, LA might inhibit the biosynthesis of arginine, resulting in the dysfunction of arginine metabolism, which causes the accumulation of intracellular ROS in bacteria. Furthermore, the expression of cold shock protein is up-regulated in bacteria to relieve antibiotic pressure (Chanda et al., 2010). The expression of cold shock protein was also up-regulated in MRSA treated by LA (shown in Table 2), indicating that LA also caused the antibiotic pressure on MRSA.

### 3.5. Application of GA@LA micelles on pork preservation

The size distribution of micelles is measured by using dynamic light scattering (DLS). Compared to GA micelles, GA@LA micelles showed larger size distribution and greater diameters (shown in Fig. 3B). As shown in Fig. 6C, the particle sizes of GA and GA@LA micelles were 104.6 nm and 167.3 nm, respectively. Meanwhile, the polymer dispersity index (shown in Fig. 6E) of GA and GA@LA micelles were 0.130 and 0.256 respectively, which might have contributed to the encapsulation of LA. The polymer dispersity index of GA and GA@LA micelles were less than 0.3, indicating that the prepared nano-micelles had acceptable homogeneity. The zeta potentials of GA and GA@LA micelles were − 1.32 mV and − 29.3 mV (shown in Fig. 6D), indicating that micelles had a negative surface charge. Micelles become more stable when their absolute potential increases (Shen et al., 2021). Compared with the zeta potentials of GA and GA@LA micelles, the absolute potential of GA@LA micelle was about 22-times that of GA micelles, indicating that GA@LA micelle was more stable. The TEM images (shown in Fig. 6F) demonstrated that GA and GA@LA micelles were spherical. As shown in Fig. 6G, compared with the control group and GA micelle group, GA@LA micelles showed potent activities against MRSA, where there were no visible colonies on the culture plates. Meanwhile, the model of fresh pork contamination by MRSA was constructed and displayed in Fig. 6H and I. In the control group, the count of MRSA ranged from 6.6 to 5.4 $\log_{10}$CFU/mL when the fresh pork was stored at 4 °C for 7 days. However, in the GA@LA micelles group, the value of $\log_{10}$CFU/mL remained zero when the fresh pork was stored at 4 °C for 7 days. This was consistent with the above results that GA@LA micelles showed potent inhibition on the growth of MRSA and exhibited the potential to protect the pork contamination caused by MRSA. GA has great potential in drug delivery, due to its ability to self-associate with the formation of a “host-guest” type complex, where the host is GA and the guest is a loaded compound (Selyutina & Polyakov, 2019). For example, GA served as a drug delivery system to improve the solubility and bioavailability of quercetin (Olchowik-Grabarek et al., 2023).

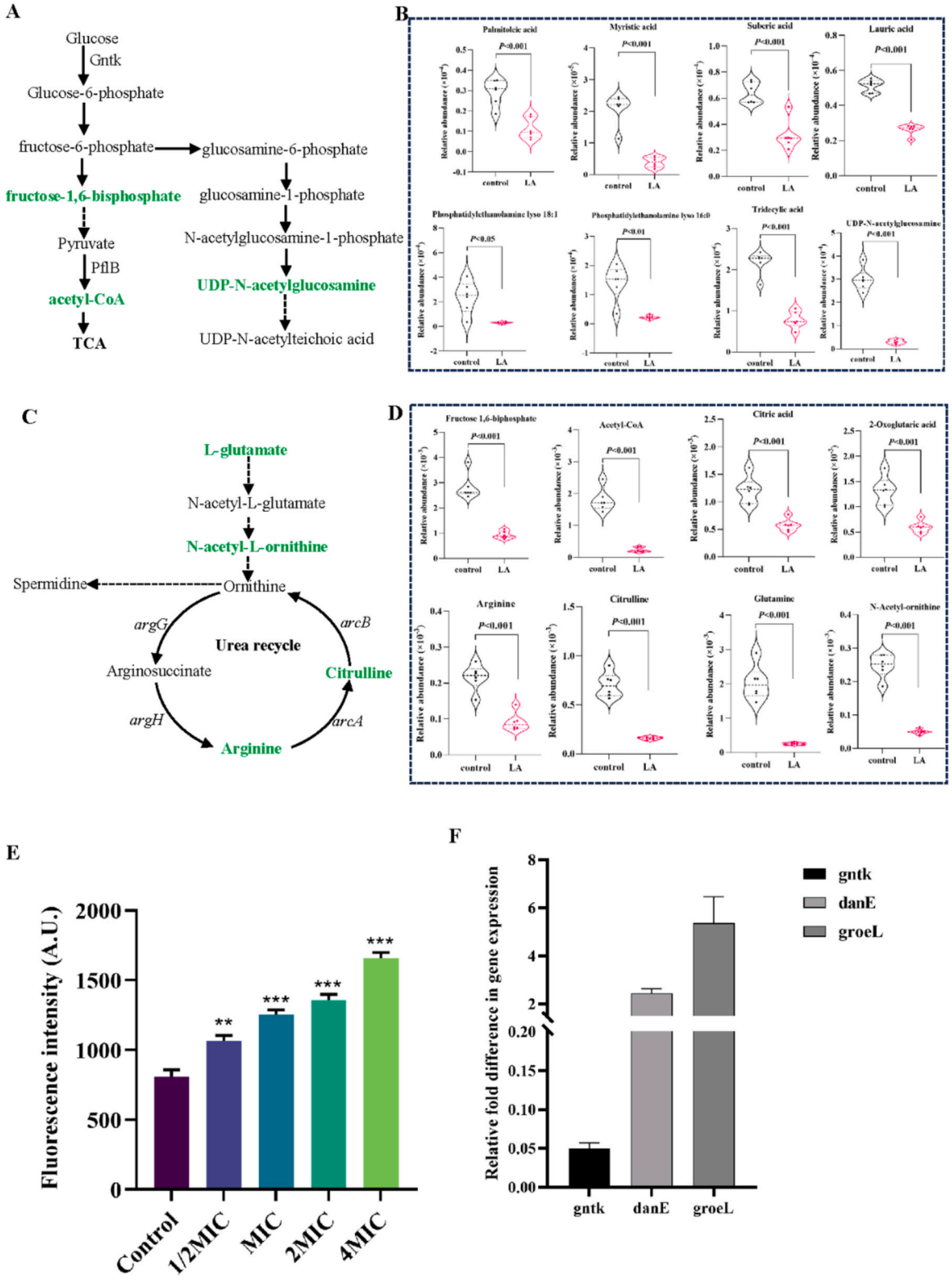


**Fig. 3.** (**A**) Diagram of glycolysis and TCA cycle pathway; (**B**)The major differential metabolites in the synthesis of fatty acids; (**C**) Diagram of arginine and urea recycle; (**D**) The major differential metabolites in the arginine metabolism; (**E**) The effects of LA on the production of ROS in MRSA; (**F**) The RT-PCR results of related genes; $^{*}P < 0.05$, $^{**}P < 0.01$, $^{***}P < 0.001$, LA group vs control group.

## 4. Conclusions

The isopentenyl flavonoids derived from Glycyrrhiza inflata have demonstrated significant efficacy against MRSA. Concurrently, licochalcone A (LA) was observed to disrupt arginine metabolism in MRSA, potentially leading to intracellular ROS accumulation. Additionally, LA was found to inhibit glucokinase expression in the Embden-Meyerhof-Parnas (EMP) pathway, which might impede the synthesis of ATP, fatty acids, and peptidoglycan. Although the mechanism of LA's action against MRSA appears to involve targeting arginine and carbohydrate

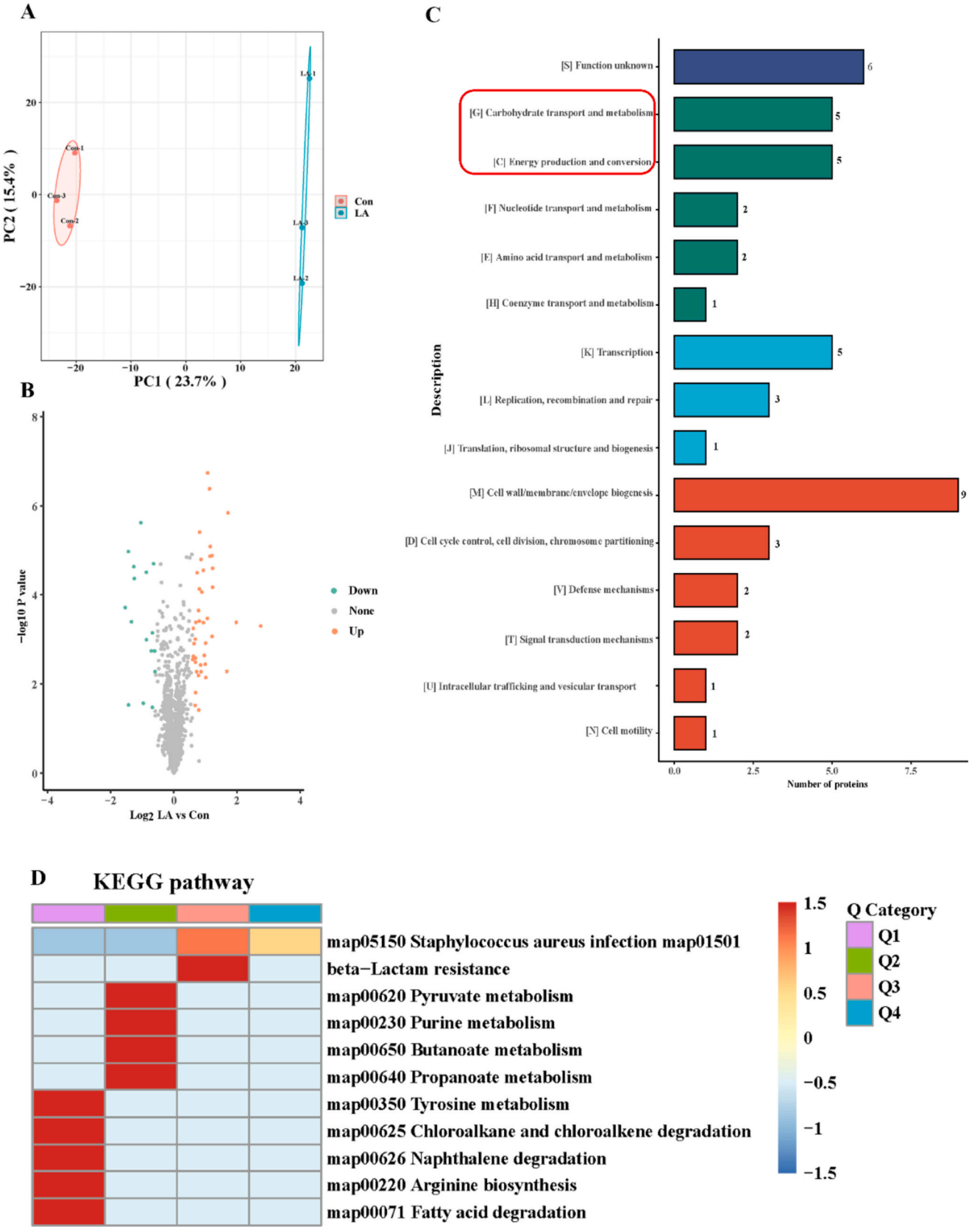


**Fig. 4.** (**A**) Principal component analysis of the proteome; **(B)** The volcano plot of differentially expressed proteins between control and MRSA treated by LA; **(C)** COG/KOG category of identified DEPs in MRSA treated by LA; **(D)** The KEGG pathway analysis of differentially expressed proteins.

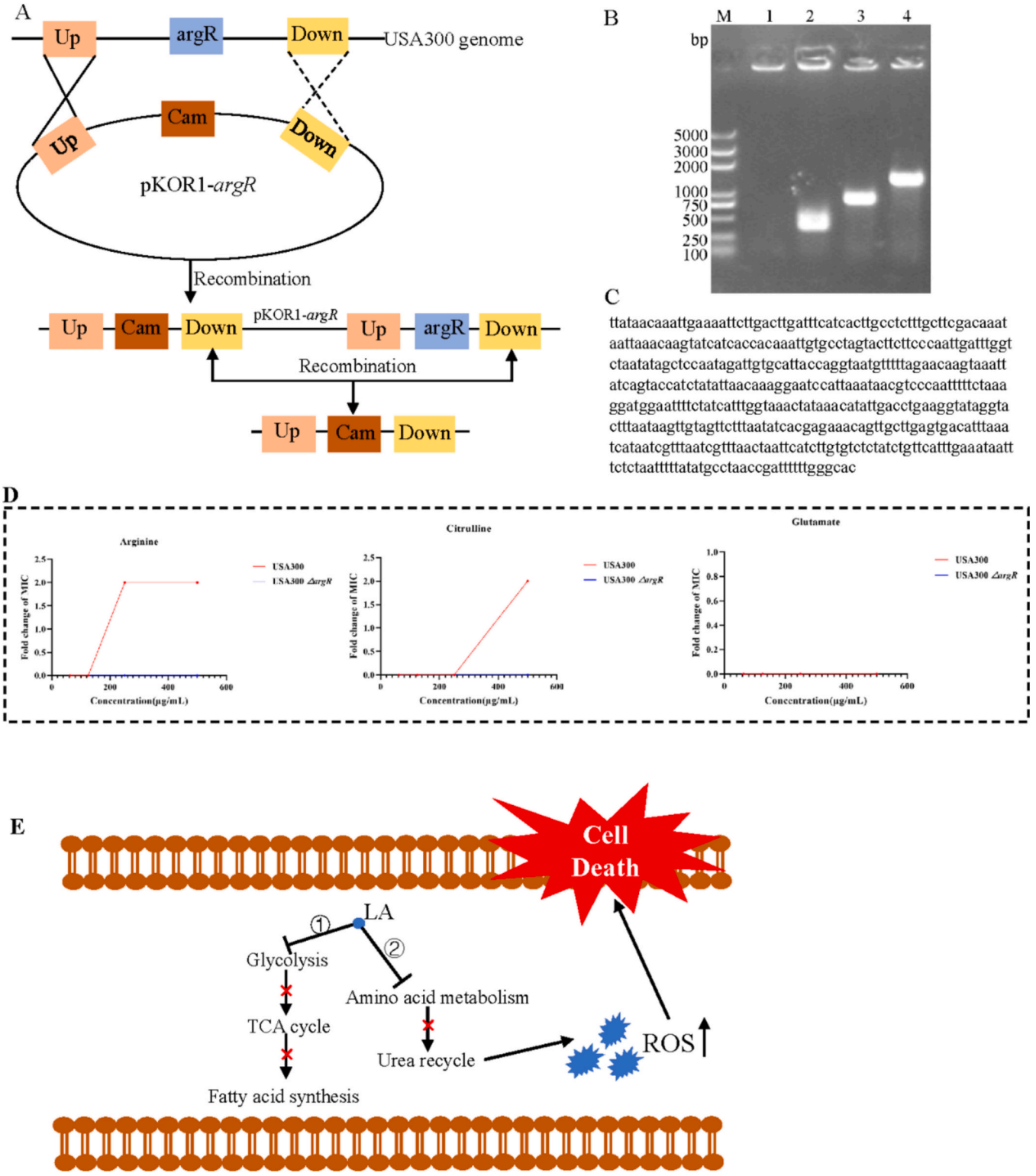


**Fig. 5.** **(A)** The construction of USA300△*argR* by using allelic replacement; **(B)** The identification of USA300△*argR*, M:5000 bp DNA Ladder, lane1: PCR production in USA300△*argR* by using primer of argR-ter-F/R, lane2: PCR production in USA300 by using primer of argR-ter-F/R, lane3: PCR production in USA300△*argR* by using primer of argR-JD-F/R, lane4: PCR production in USA300 by using primer of argR-JD-F/R; **(C)** The sequence of deleted gene in USA300△*argR*; **(D)** The effects of exogenous addition of arginine, citrulline and glutamate on MIC of LA against USA300 or USA300△*argR*; **(E)** The potential actions of LA against MRSA.

metabolism, further studies are required to elucidate how LA inhibits glucokinase expression and affects arginine metabolism in MRSA. Moreover, GA could be used as carrier to improve the solubility of LA, and the complex of GA loaded with LA has the potential to prevent fresh pork from being contaminated by MRSA.

**Funding**

This research was funded by the Hubei Provincial Natural Science Foundation (No.2023AFB403), Hubei Provincial Department of Education Project (Q2022007) and was also supported by 2023 Outstanding

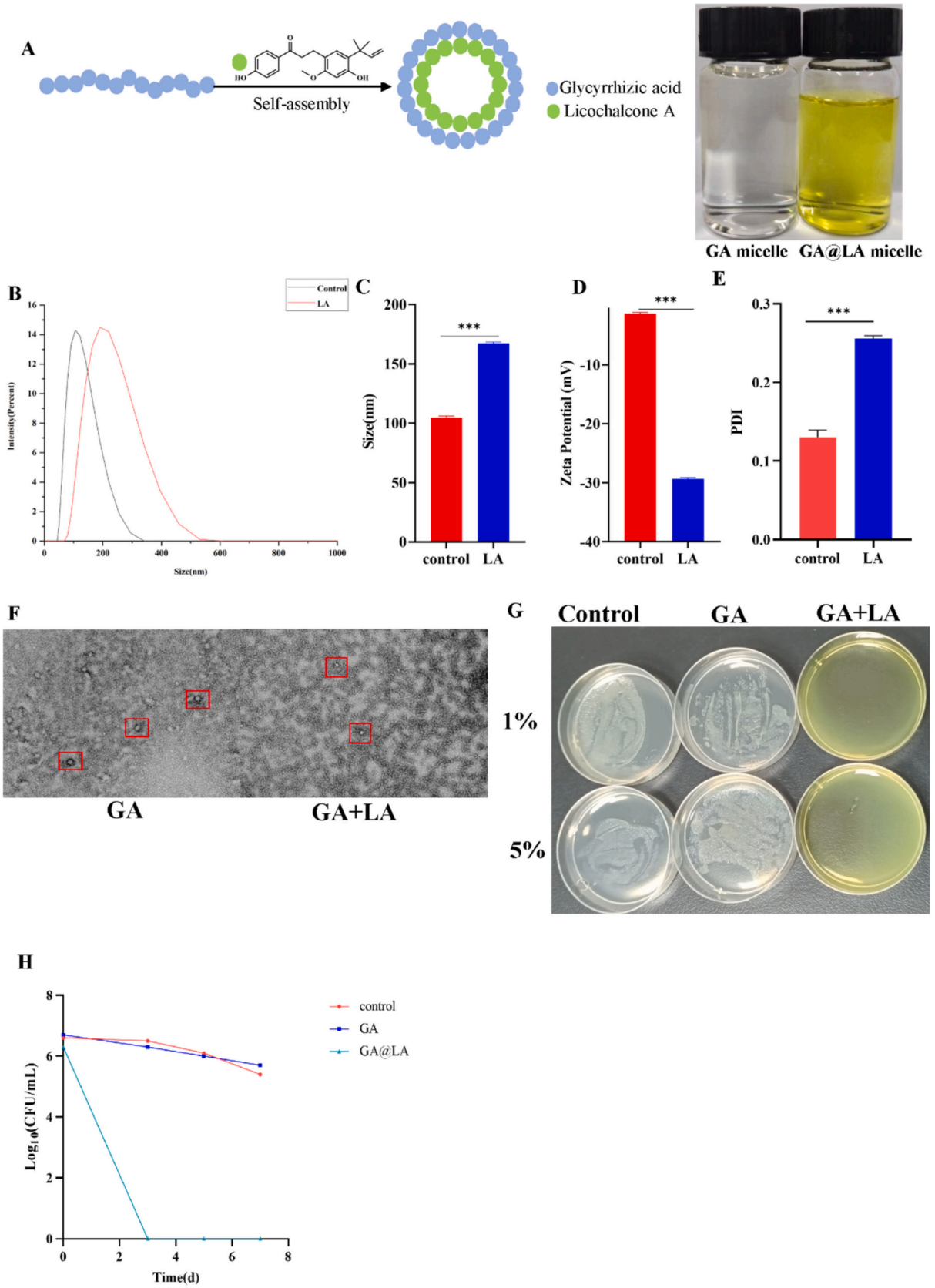


**Fig. 6.** **(A)** Self-assembly of nano micelles; **(B–C)** The particle size of GA and GA@LA micelles; **(D)** The zeta potentials of GA and GA@LA micelles; **(E)** The polymer dispersity index of GA and GA@LA micelles; **(F)** The TEM images of GA and GA@LA micelles; **(G)** The antibacterial activities of GA and GA@LA micelles; **(H)** The effects of GA and GA@LA micelles on the fresh pork preservation.

Young Science and Technology Talents (Innovation) Training Special Project (No.XJ2023001602).

## Informed consent statement

Not applicable.

## CRediT authorship contribution statement

**Fei Zeng:** Project administration, Investigation, Funding acquisition, Formal analysis, Data curation, Conceptualization. **Shijuan Shao:** Writing – review & editing, Writing – original draft, Methodology, Conceptualization. **Zhilu Zou:** Writing – review & editing, Funding acquisition. **Siqi Guo:** Data curation. **Yu Cai:** Data curation. **Chunchao Yan:** Methodology. **Yunzhong Chen:** Investigation. **Maolin Wang:** Funding acquisition, Conceptualization. **Tingting Shi:** Writing – review & editing, Writing – original draft.

## Declaration of competing interest

The authors declare that they have no known competing financial interests or personal relationships that could have appeared to influence the work reported in this paper.

## Data availability

Data will be made available on request.

## Appendix A. Supplementary data

Supplementary data to this article can be found online at https://doi.org/10.1016/j.fochx.2024.101893.

## References


Andrews, J. M. (2001). Determination of minimum inhibitory concentrations. *Journal of Antimicrobial Chemotherapy, 48*(1), 5–16.

Chanda, P. K., Bandhu, A., Jana, B., Mondal, R., Ganguly, T., Sau, K., … Sau, S. (2010). Characterization of an unusual cold shock protein from *Staphylococcus aureus*. *Journal of Basic Microbiology, 50*(6), 519–526.

Chen, L., Kan, J., Zheng, N., Li, B., Hong, Y., Yan, J., … Li, H. (2021). A botanical dietary supplement from white peony and licorice attenuates nonalcoholic fatty liver disease by modulating gut microbiota and reducing inflammation. *Phytomedicine, 91*, Article 153693.

Cheng, C., Dong, Z., Han, X., Sun, J., Wang, H., Jiang, L., Yang, Y., Ma, T., Chen, Z., Yu, J., Fang, W., & Song, H. (2017). *Listeria monocytogenes* 10403S arginine repressor ArgR finely tunes arginine metabolism regulation under acidic conditions. *Frontiers in Microbiology, 8*, 143.

Cheung, G. Y. C., Bae, J. S., & Otto, M. (2021). Pathogenicity and virulence of Staphylococcus aureus. *Virulence, 12*(1), 547–569.

Cunin, R., Glansdorff, N., Piérard, A., & Stalon, V. (1987). Biosynthesis and metabolism of arginine in bacteria. *Microbiological Reviews, 50*(3), 314–352.

Davidov-Pardo, G., Joye, I. J., & Mcclements, D. J. (2015). Food-grade protein-based nanoparticles and microparticles for bioactive delivery: Fabrication, characterization, and utilization. *Advances in Protein Chemistry and Structural Biology, 98*, 293–325.

Hernández-Aristizábal, I., & Ocampo-Ibáñez, I. D. (2021). Antimicrobial peptides with antibacterial activity against vancomycin-resistant *staphylococcus aureus* strains: Classification, structures, and mechanisms of action. *International Journal of Molecular Sciences, 22*(15), 7927.

Kang, S., Kong, F., Liang, X., Li, M., Yang, N., Cao, X., … Zheng, Y. (2019). Label-free quantitative proteomics reveals the multitargeted antibacterial mechanisms of Lactobionic acid against methicillin-resistant *Staphylococcus aureus* (MRSA) using SWATH-MS technology. *Journal of Agricultural and Food Chemistry, 67*(44), 12322–12332.

Kim, S. J., Chang, J., & Singh, M. (2015). Peptidoglycan architecture of Gram-positive bacteria by solid-state NMR. *Biochimica et Biophysica Acta Biomembranes, 1848*(1 Pt B), 350–362.

Lunde, C. S., Hartouni, S. R., Janc, J. W., Mammen, M., Humphrey, P. P., & Benton, B. M. (2009). Telavancin disrupts the functional integrity of the bacterial membrane through targeted interaction with the cell wall precursor lipid II. *Antimicrobial Agents and Chemotherapy, 53*(8), 3375–3383.

Michael, A. J. (2018). Polyamine function in archaea and bacteria. *Journal of Biological Chemistry, 293*(48), 18693–18701.

Ning, H., Wang, S., Li, Y., Sun, G., & He, J. (2021). The cell structure damage and embden-meyerhof-parnas pathway inhibition of *Listeria monocytogenes* induced by glycinin basic peptide. *Microbial Pathogenesis, 293*(48), 18693–18701.

Olchowik-Grabarek, E., Czerkas, K., Matchanov, A. D., Esanov, R. S., Matchanov, U. D., Zamaraeva, M., & Sekowski, S. (2023). Antibacterial and Antihemolytic activity of new biomaterial based on Glycyrrhizic acid and quercetin (GAQ) against *Staphylococcus aureus*. *Journal of Functional Biomaterials, 14*(7), 368.

Otto, C. C., Cunningham, T. M., Hansen, M. R., & Haydel, S. E. (2010). Effects of antibacterial mineral leachates on the cellular ultrastructure, morphology, and membrane integrity of *Escherichia coli* and methicillin-resistant *Staphylococcus aureus*. *Annals of Clinical Microbiology and Antimicrobials, 16*(9), 26.

Papadopoulos, P., Angelidis, A. S. T., Kotzamanidis, C., Zdragas, A., Papa, A., Filioussis, G., & Sergelidis, D. (2019). *Staphylococcus aureus* and methicillin-resistant *S. aureus* (MRSA) in bulk tank milk, livestock and dairy-farm personnel in north-central and North-Eastern Greece: Prevalence, characterization and genetic relatedness. *Food Microbiology, 84*, Article 103249.

Parsons, J. B., & Rock, C. O. (2011). Is bacterial fatty acid synthesis a valid target for antibacterial drug discovery? *Current Opinion in Microbiology, 14*(5), 544–549.

Qu, D., Hou, Z., Li, J., Luo, L., Su, S., Ye, Z., Bai, Y., Zhang, X., Chen, G., Li, Z., Wang, Y., Xue, X., Luo, X., & Li, M. (2020). A new coumarin compound DCH combats methicillin-resistant *Staphylococcus aureus* biofilm by targeting arginine repressor. *Science Advances, 6*(30), Article eaay9597.

Selyutina, O. Y., & Polyakov, N. E. (2019). Glycyrrhizic acid as a multifunctional drug carrier - from physicochemical properties to biomedical applications: A modern insight on the ancient drug. *International Journal of Pharmaceutics, 559*, 271–279.

da Silva, A. C., Rodrigues, M. X., & Silva, N. C. C. (2020). Methicillin-resistant *Staphylococcus aureus* in food and the prevalence in Brazil: A review. *Brazilian Journal of Microbiology, 51*(1), 347–356.

Shen, C., Shen, B., Zhu, J., Wang, J., Yuan, H., & Li, X. (2021). Glycyrrhizic acid-based self-assembled micelles for improving oral bioavailability of paeoniflorin. *Drug Development and Industrial Pharmacy, 47*(2), 207–214.

Song, M., Liu, Y., Li, T., Liu, X., Hao, Z., Ding, S., … Shen, J. (2021). Plant natural flavonoids against multidrug resistant pathogens. *Advanced Science, 8*(15), Article e2100749.

Soontornpas, C., Saraya, S., Chulasiri, M., Chindavijak, B., & Mootsikapun, P. (2005). Time-kill curves as a tool for targeting ceftazidime serum concentration during continuous infusion for treatment of septicaemic melioidosis. *International Journal of Antimicrobial Agents, 26*(5), 403–407.

Su, H. L., Chou, C. C., Hung, D. J., Lin, S. H., Pao, I. C., Lin, J. H., … Lin, J. J. (2009). The disruption of bacterial membrane integrity through ROS generation induced by nanohybrids of silver and clay. *Biomaterials, 30*(30), 5979–5987.

Sudhamsu, J., & Crane, B. R. (2009). Bacterial nitric oxide synthases: What are they good for? *Trends in Microbiology, 17*(5), 212–218.

Sun, A., Huang, Z., He, L., Dong, W., Tian, Y., Huang, A., & Wang, X. (2023). Metabolomic analyses reveal the antibacterial properties of a novel antimicrobial peptide MOp3 from *Moringa oleifera* seeds against *Staphylococcus aureus* and its application in the infecting pasteurized milk. *Food Control, 150*.

Sun, X., Duan, X., Wang, C., Liu, Z., Sun, P., Huo, X., Ma, X., Sun, H., Liu, K., & Meng, Q. (2017). Protective effects of glycyrrhizic acid against non-alcoholic fatty liver disease in mice. *European Journal of Pharmacology, 806*, 75–82.

Vimala, A., & Harinarayanan, R. (2016). Transketolase activity modulates glycerol-3-phosphate levels in *Escherichia coli*. *Molecular Microbiology, 100*(2), 263–277.

Vollmer, W., Blanot, D., & De Pedro, M. A. (2008). Peptidoglycan structure and architecture. *FEMS Microbiology Reviews, 32*(2), 149–167.

Weng, Z., Zeng, F., Wang, M., Guo, S., Tang, Z., Itagaki, K., … Wang, F. (2023). Antimicrobial activities of lavandulylated flavonoids in Sophora flavences against methicillin-resistant *Staphylococcus aureus* via membrane disruption. *Journal of Advanced Research, S2090-1232*(23), 00123-6.

Yu, H. H., Chin, Y. W., & Paik, H. D. (2021). Application of natural preservatives for meat and meat products against food-borne pathogens and spoilage bacteria: A review. *Foods, 10*(10), 2418.

Zeng, F., Weng, Z., Zheng, H., Xu, M., Liang, X., & Duan, J. (2021). Preparation and characterization of active oxidized starch films containing licorice residue extracts and its potential against methicillin-resistant *S. aureus*. *International Journal of Biological Macromolecules, 187*, 858–866.

Zeng, Q., Wang, Z., Zhu, Z., Hu, Y., Wang, Y., Xue, Y., Wu, Y., Guo, Y., Liang, P., Chen, H., Zheng, Z., Shen, C., Jiang, C., Zhu, H., Shen, Q., Yi, Y., Li, H., Yang, Z., Liu, L., & Liu, Q. (2022). Glycyrrhizin micellar nanocarriers for topical delivery of baicalin to the hair follicles: A targeted approach tailored for alopecia treatment. *International Journal of Pharmaceutics, 625*, Article 122109.

Zhu, Y., Peng, W., Zhang, J., Wang, M., Firempong, C. K., Feng, C., … Yu, J. (2014). Enhanced oral bioavailability of capsaicin in mixed polymeric micelles: Preparation, in vitro and in vivo evaluation. *Journal of Functional Foods, 8*, 358–366.